

Forced Convection in a Circular Pipe with a Partially Filled Porous Medium

Woo Tae Kim*, Ki Hyuck Hong, Myung S. Jhon

Department of Chemical Engineering & Data Storage Systems Center, Carnegie Mellon University,
5000 Forbes Ave., Pittsburgh, PA 15213-3890

John G. VanOsdol, Duane H. Smith

National Energy Technology Laboratory, U.S. Department of Energy,
3610 Collins Ferry Rd., Morgantown, WV 26509-0880

A study of forced convection in a circular pipe with a partially filled porous medium was numerically investigated. The Brinkman-Forchheimer extension of the Darcy model was used to analyze the and temperature distribution in the porous medium. Our study includes two types of porous layer configurations: (1) a layer attached at the tube wall extending inward towards the centerline and (2) a layer at the centerline extending outward. The effect of several parameters, such as Darcy number, effective viscosity, effective thermal conductivity, and inertia parameter, as well as the effect of geometric parameters, were investigated.

Key Words: Forced Convection, Porous Medium, Brinkman-Forchheimer Equation, Darcy Model

Nomenclature

Roman Symbols

c_F : Forchheimer coefficient
 c_P : Specific heat at constant pressure
 Da : Darcy number
 F : Forchheimer number
 I_0 : Modified Bessel function of the first kind of order zero
 I_1 : Modified Bessel function of the first kind of order one
 k : Thermal conductivity
 k_{eff} : Effective thermal conductivity of the porous layer
 K : Permeability of the porous medium
 K_0 : Modified Bessel function of the second kind of order zero
 K_1 : Modified Bessel function of the second kind of order one

Nu : Nusselt number
 p : Pressure
 q : Heat flux
 r, \hat{r} : Non-dimensional radial coordinate
 R : Radius of the circular pipe
 R_0 : Location of the interface between the fluid and the porous medium
 R_k : Ratio of the effective thermal conductivity of the porous layer to the thermal conductivity of the fluid
 R_μ : Ratio of the effective viscosity of the porous layer to the viscosity of the fluid
 T^* : Temperature
 T_m : Average temperature
 T_w : Wall temperature
 u, \hat{u} : Non-dimensional axial velocity component of the fluid
 u_m : Average velocity
 x : Non-dimensional axial coordinate

* Corresponding Author,

E-mail : mj3a@andrew.cmu.edu

TEL : +1-412-268-2233; FAX : +1-412-268-7139

Department of Chemical Engineering & Data Storage Systems Center, Carnegie Mellon University, 5000 Forbes Ave., Pittsburgh, PA 15213-3890. (Manuscript Received March 24, 2003; Revised July 10, 2003)

Greek Symbols

μ : Fluid viscosity
 μ_{eff} : Effective viscosity of the porous layer
 ρ : Fluid density

θ : Non-dimensional temperature

Subscripts

eff : Effective values

m : Average values

w : Values at the wall

Superscript

*

1. Introduction

The study of the characteristics of heat and momentum convection in porous media has increased significantly due to its relevance in a variety of technology, including the design of ceramic barrier filter systems exposed to high temperatures (Ahmadi and Smith, 2002a, 2002b, 1998; Back et al., 1997), superadiabatic combustion (Jeong et al., 1998), fuel cell applications (Nguyen and He, 2002; He et al., 2000), and membrane science and technology (Mckenzie et al., 1994; Webber et al., 1990).

Forced-convection heat transfer in a channel or a tube partially filled or saturated with porous media is of mathematical and practical interest. Kaviany (1985) analyzed heat transfer in a channel filled with porous media using an equation based on the Brinkman-extended Darcy flow model. Vafai and Kim (1989) reported an exact solution of that equation, including inertia (Brinkman-Forchheimer extended Darcy equation) for convective heat transfer in a channel with uniform wall heat flux under the boundary layer assumption. Analytic solutions of the Brinkman-Forchheimer equation and associated heat transfer equation for a plane channel were reported by Nield et al. (1996), where they investigated the effect of several parameters, including effective viscosity, Darcy number, and Forchheimer number.

Poulikakos and Kazmierczak (1987) investigated the forced convection in a channel and a circular pipe partially filled with porous medium. Specifically, they studied the effects of the porous layer thickness, Darcy number, and effective thermal conductivity of the porous media on heat transfer through exact solutions of the Brink-

man-extended Darcy and energy equations. Their analysis, however, was limited to the case where the effective viscosity of the porous medium was equal to the fluid viscosity. Poulikakos and Renken (1987) also investigated the forced convection in a channel, including the effects of flow inertia, variable porosity, and friction. A similar solution was obtained by Ethier and Kamm (1989) for flow in a circular pipe partially filled with porous medium.

In this paper, we examined the effect of several parameters on forced convection in a tube partially filled with a porous medium. Since there is no analytic solution for the Brinkman-Forchheimer extension of Darcy momentum equation in a circular pipe, we performed a numerical calculation.

In particular, we have investigated the effects of porous layer configuration; a layer attached to the tube wall extending inward toward the center line (Case I), and a layer extending outward from the center line (Case II). The effects of other parameters, such as Darcy number, the porous layer thickness, effective viscosity, effective thermal conductivity of the porous media, and Forchheimer number were also investigated. A finite difference method was adopted with the boundary conditions of both constant wall temperature (Dirichlet type) and constant wall heat flux (Neumann type).

2. Formulation

Schematics of the physical model and coordinate system are shown in Fig. 1(a) for the Case I and in Fig. 1(b) for the Case II. The location of the interface between the fluid and the porous medium is R and the pipe radius is R_0 . The

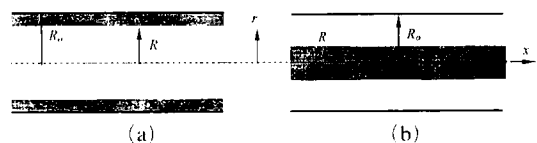


Fig. 1 Schematics of the physical model and coordinate system : (a) outer porous layer (Case I) and (b) inner porous layer (Case II)

porous layer has an effective viscosity μ_{eff} and an effective thermal conductivity k_{eff} , while the fluid has viscosity μ and thermal conductivity k . For the flow system shown in Fig. 1, a steady, incompressible, hydrodynamic and thermal laminar flow is assumed.

The governing equations for the velocity and temperature fields in the fluid layer can be written in dimensional form as

$$\frac{dp}{dx^*} = \frac{1}{r^*} \frac{d}{dr^*} \left(\mu r^* \frac{du^*}{dr^*} \right) \tag{1}$$

$$\rho c_p u^* \frac{dT^*}{dx^*} = \frac{1}{r^*} \frac{d}{dr^*} \left(k r^* \frac{dT^*}{dr^*} \right) \tag{2}$$

The Brinkman-Forchheimer extended Darcy and energy equations are used to the flow in the porous region and are given by

$$\frac{dp}{dx^*} = \mu_{eff} \frac{1}{r^*} \frac{d}{dr^*} \left(r^* \frac{du^*}{dr^*} \right) - \frac{\mu}{K} u^* - \frac{c_F \rho}{\sqrt{K}} u^{*2} \tag{3}$$

$$\rho c_p u^* \frac{dT^*}{dx^*} = k_{eff} \frac{1}{r^*} \frac{d}{dr^*} \left(r^* \frac{dT^*}{dr^*} \right) \tag{4}$$

In deriving Eq. (4), a homogeneous isotropic porous medium is assumed. At any point in the porous medium, the solid matrix is assumed to be in thermal equilibrium with the fluid filling the pores (Bejan, 1995). Heat conduction in the axial direction is neglected under a low Peclet number assumption. Note that the effect of thermal dispersion is not considered in the energy equation, since we take into account the effect of thermal dispersion by modifying the thermal conductivity (Vafai and Kim, 1989; Nield et al., 1996).

The appropriate boundary conditions for the momentum and energy equations (Eqs. (1) ~ (4)) are given :

At $r^* = 0$,

$$\frac{du^*}{dr^*} = 0 \text{ and } \frac{dT^*}{dr^*} = 0 \text{ for Cases I and II} \tag{5}$$

At $r^* = R_0$,

$$u^* = 0, T^* = T_w \text{ or } \frac{dT^*}{dr^*} = \frac{q_w}{k_{eff}} \text{ for Case I} \tag{6}$$

$$u^* = 0, T^* = T_w \text{ or } \frac{dT^*}{dr^*} = \frac{q_w}{k} \text{ for Case II}$$

In addition to the conditions of continuity of velocity and temperature at the interface, the following matching conditions at the fluid/porous interface ($r^* = R$) are imposed :

$$\mu \frac{du^*}{dr^*} = \mu_{eff} \frac{du^*}{dr^*}$$

$$k \frac{dT^*}{dr^*} = k_{eff} \frac{dT^*}{dr^*} \tag{7}$$

These boundary conditions represent the continuity of shear stress and heat flux at the interface. By introducing the non-dimensional variables defined by :

$$\hat{r} = \frac{r^*}{\sqrt{K}}, \hat{R} = \frac{R}{\sqrt{K}}, \hat{R}_0 = \frac{R_0}{\sqrt{K}}$$

$$u = \frac{u^*}{-\frac{1}{\mu} \left(\frac{dp}{dx^*} \right) R_0^2} \tag{8}$$

where K is the permeability of the porous medium. The non-dimensional parameters for the ratio of the effective viscosity of the porous layer to the viscosity of the fluid (R_μ), Darcy number (Da) and Forchheimer number (F) defined by :

$$R_\mu = \frac{\mu_{eff}}{\mu}, Da = \frac{K}{R_0^2}$$

$$F = \frac{c_F \rho \left(-\frac{dp}{dx^*} \right) R_0^4}{\sqrt{K} \mu^2} \tag{9}$$

the momentum equations for the fluid (Eq. (1)) and porous (Eq. (3)) regions become

$$\frac{d^2 u}{d\hat{r}^2} + \frac{1}{\hat{r}} \frac{du}{d\hat{r}} = -Da \tag{10}$$

$$\frac{d^2 u}{d\hat{r}^2} + \frac{1}{\hat{r}} \frac{du}{d\hat{r}} - \frac{1}{R_\mu} u = \frac{1}{R_\mu} Da (Fu^2 - 1) \tag{11}$$

For the case of a vanishing permeability, $K=0$ (or $Da=0$), the velocity in the porous region is equal to zero from Eq. (3). At the limit of $Da \rightarrow \infty$, Eq. (3) has the same form as the momentum equation in the fluid region except the effective viscosity.

If $R_\mu=1$ and $F=0$, we can obtain an analytic solution. The solution for Case I becomes (Ethier and Kamm, 1989)

$$u = Da[A_1 - \hat{r}^2/4] \quad \text{fluid region} \quad (12)$$

$$u = Da[1 + B_1 I_0(\hat{r}) + B_2 K_0(\hat{r})] \quad \text{porous region} \quad (13)$$

Here, I_0 and K_0 are modified Bessel functions of the first and second kind of order zero. The constants A_1 , B_1 , and B_2 are given as :

$$A_1 = 1 + \hat{R}^2/4 + B_1 I_0(\hat{R}) + B_2 K_0(\hat{R}) \quad (14)$$

$$B_1 = -\frac{K_1(\hat{R}) + (\hat{R}/2) K_0(\hat{R}_0)}{I_0(\hat{R}_0) K_1(\hat{R}) + K_0(\hat{R}_0) I_1(\hat{R})} \quad (15)$$

$$B_2 = -\frac{I_1(\hat{R}) - (\hat{R}/2) I_0(\hat{R}_0)}{I_0(\hat{R}_0) K_1(\hat{R}) + K_0(\hat{R}_0) I_1(\hat{R})} \quad (16)$$

where I_1 and K_1 are modified Bessel functions of the first and second kind of order one.

For the Case II, we can obtain the velocity profile solution for $R_\mu=1$ and $F=0$,

$$u = Da[\hat{R}_0^2 - \hat{r}^2]/4 + C_1 \ln(\hat{r}/\hat{R}_0) \quad \text{fluid region} \quad (17)$$

$$u = Da[1 + D_1 I_0(\hat{r})] \quad \text{porous region} \quad (18)$$

where

$$C_1 = Da\hat{R}[B_1 I_1(\hat{R}) + \hat{R}/2] \quad (19)$$

$$D_1 = \frac{(\hat{R}_0^2 - \hat{R}^2)/4 - 1 + \hat{R}^2 \ln(\hat{R}/\hat{R}_0)/2}{I_0(\hat{R}) - \hat{R} I_1(\hat{R}) \ln(\hat{R}/\hat{R}_0)} \quad (20)$$

If $R_\mu \neq 1$ or $F \neq 0$, we are unable to obtain an analytic solution, and therefore perform a numerical approach. Equations (12) ~ (20) are also used to verify the accuracy of the finite difference scheme.

By introducing the non-dimensional radius (r), velocity (\hat{u}), temperature (θ) and Nusselt number (Nu) given by

$$\begin{aligned} r &= \frac{r^*}{R_0}, \quad \hat{u} = \frac{u^*}{u_m}, \quad \theta = \frac{T^* - T_w}{T_m - T_w}, \\ Nu &= \frac{2R_0}{k} \frac{q_w}{T_w - T_m} \end{aligned} \quad (21)$$

where average velocity u_m and average temperature T_m are defined by

$$\begin{aligned} u_m &= \frac{2}{R_0^2} \int_0^{R_0} u^* r^* dr^* \\ T_m &= \frac{2}{R_0^2 u_m} \int_0^{R_0} u^* T^* r^* dr^* \end{aligned} \quad (22)$$

the energy equations become

$$\frac{1}{Nu} \left[\frac{d^2 \theta}{dr^2} + \frac{1}{r} \frac{d\theta}{dr} \right] = -\hat{u} \quad \text{fluid region} \quad (23)$$

$$\frac{1}{Nu} \left[\frac{d^2 \theta}{dr^2} + \frac{1}{r} \frac{d\theta}{dr} \right] = -\hat{u} \frac{1}{R_k} \quad \text{porous region} \quad (24)$$

in the constant wall heat flux case. Here, $R_k = k_{eff}/k$ represents the ratio of effective thermal conductivity of the porous layer to the thermal conductivity of the fluid. For constant wall temperature cases, the non-dimensional temperature is multiplied into the right hand sides of Eqs. (23) and (24).

$$\frac{1}{Nu} \left[\frac{d^2 \theta}{dr^2} + \frac{1}{r} \frac{d\theta}{dr} \right] = -\hat{u} \theta \quad \text{fluid region} \quad (25)$$

$$\frac{1}{Nu} \left[\frac{d^2 \theta}{dr^2} + \frac{1}{r} \frac{d\theta}{dr} \right] = -\hat{u} \theta \frac{1}{R_k} \quad \text{porous region} \quad (26)$$

Equations (23) ~ (26) must be solved via the following boundary conditions

$$\theta|_{r=1} = 0 \quad \text{and} \quad \left. \frac{d\theta}{dr} \right|_{r=0} = 0 \quad (27)$$

The solution procedure adopted in our study begins with a trial value for Nu , then locates the value satisfying the heat flux matching condition (7), the boundary conditions (27), and the compatibility condition

$$\int_0^1 \hat{u} \theta r \, dr = \frac{1}{2} \quad (28)$$

Notice that for the constant wall temperature case, the boundary condition (Eq. (27)) leads to the trivial solution $\theta=0$. This can be avoided by writing an expression for the temperature at the first interior node near the wall surface as a function of Nu via the following discretized compatibility condition (Nielsen et al., 1996):

$$Nu = -2 \left. \frac{d\theta}{dr} \right|_{r=1} \quad (29)$$

3. Numerical Method and Procedure

The governing Eqs. (10), (11), and (23) ~ (26) are solved via a second-order finite difference scheme, discretized in the r -direction. Simpson's integration method is applied to solve the integrals appearing in the compatibility condition (Eq. (28)) and in the definition of average velocity and temperature (Eq. (22)).

We tested the accuracy of our second-order finite difference scheme through a comparison with the exact solution for $R_\mu=1$ and $F=0$, as

shown in Fig. 2. Figure 2(a) shows the velocity profile for Case I for $R/R_0=0.8$. Figure 2(b) shows the velocity profile for Case II for $R/R_0=0.5$. These figures confirm that our numerical scheme predicts the velocity profile accurately. To test our numerical scheme for the energy equation, we calculated the limiting case of the tube with pure fluid, i.e., $R_\mu=1$, $F=0$, and $Da \rightarrow \infty$. We obtained Nu of 4.36 and 3.66 for the constant wall heat flux and constant wall temperature cases, respectively. We also calculated the limiting case of a tube filled with porous media, i.e., $R_\mu=1$, $F=0$, and $Da \rightarrow 0$. Our values for Nu converge to 8.00 and 5.78 for the constant wall heat flux and for the constant wall temperature cases, respectively, demonstrating the accuracy of our scheme.

4. Results and Discussion

The effects of physical parameters, including Da , F , R_μ , R_k , as well as geometric parameters, such as the porous layer thickness and the arrangement of the layer, which were of special interest, were investigated.

Figure 2 demonstrates that the presence of the porous layer causes the fluid velocity to decrease. This effect becomes more remarkable as the Da becomes smaller, as smaller Da corresponds to smaller permeability and hence less flow for a given pressure gradient. Although both configurations, Case I (Fig. 2(a)) and Case II (Fig. 2(b)), show qualitatively similar behavior at larger Da , the effects of the arrangement of the porous layer on the velocity profile are more significant as Da decreases. The temperature profiles for Cases I and II are shown in Fig. 3. The temperature gradient at the pipe wall is greater for Case II (Fig. 3(b)) as compared to Case I (Fig. 3(a)) for given Da . The temperature gradient becomes increasingly steep as the Da decreases, making the Nu for the Case II greater than that for Case I, as shown in Fig. 4. This demonstrates the dependence of Nu on the porous layer configuration.

The most noticeable fact in Case II (Fig. 4(b)) is the existence of maximum Nu . This is contrary

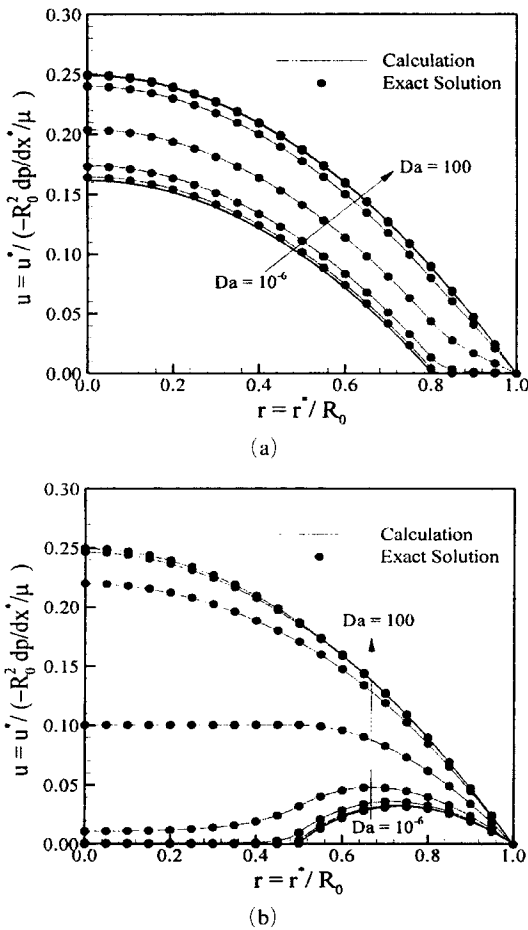
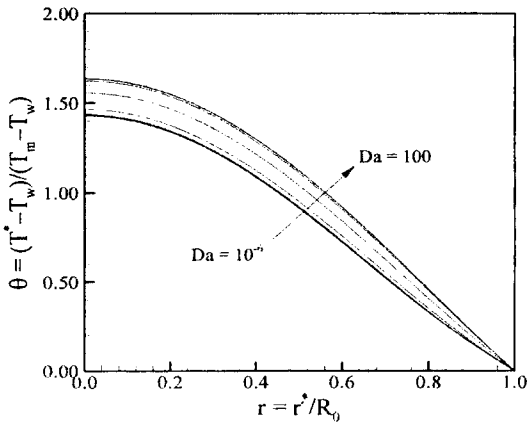
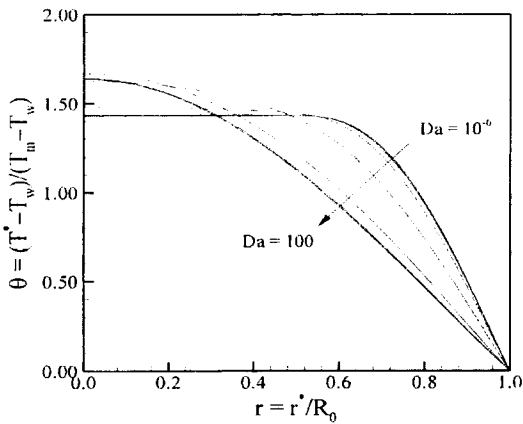


Fig. 2 Velocity profiles for the constant wall heat flux case for $F=0$ and $R_\mu=1$: (a) Case I ($R/R_0=0.8$) and (b) Case II ($R/R_0=0.5$)



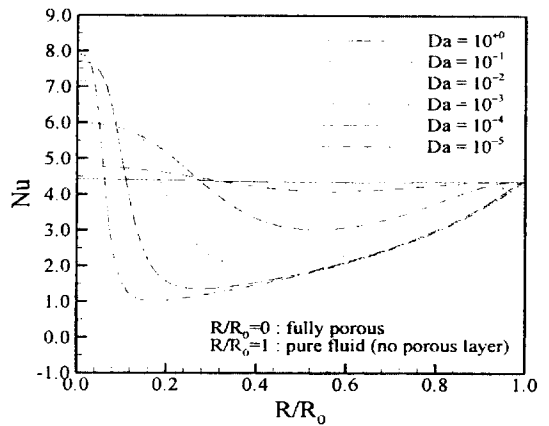
(a)



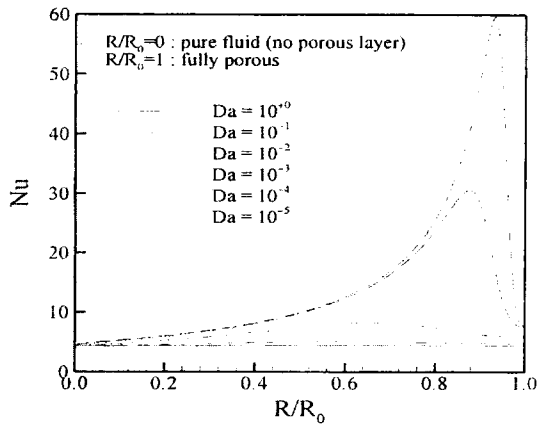
(b)

Fig. 3 Temperature profiles for the constant wall heat flux case for $F=0$: (a) Case I ($R/R_0=0.8$) and (b) Case II ($R/R_0=0.5$)

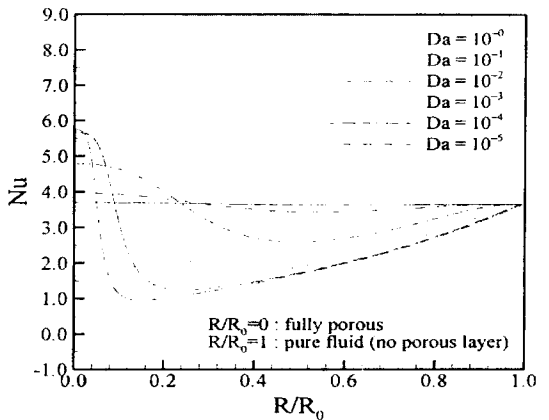
to the case I, which possesses a minimum Nu (Fig. 4(a)). Nu for Case II is larger for all values of Da and thickness of the porous layer, in contrast to Case I, due to the relatively small temperature difference ($T_w - T_m$). For Case I, Poulidakos and Kazmierczak (1987) provide an explanation for Nu dependence on the porous layer thickness. Similar rationale is applicable to Case II. As the thickness of the porous layer increases, the flow rate in the pipe decreases, and hence both T_w and T_m increase since the wall heat flux remains constant. The increasing rates of T_w and T_m , however, depend on the thickness of the porous region. When the thickness of the porous layer is small, the average temperature is



(a)



(b)



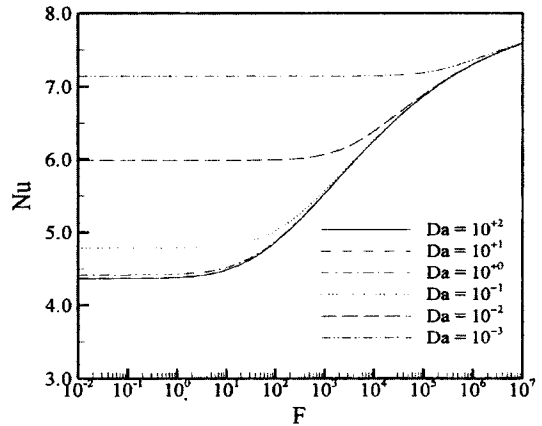
(c)

Fig. 4 Effect of porous layer thickness on Nusselt number for $F=0$: (a) Case I with constant wall heat flux, (b) Case II with constant wall heat flux, and (c) Case I with constant wall temperature

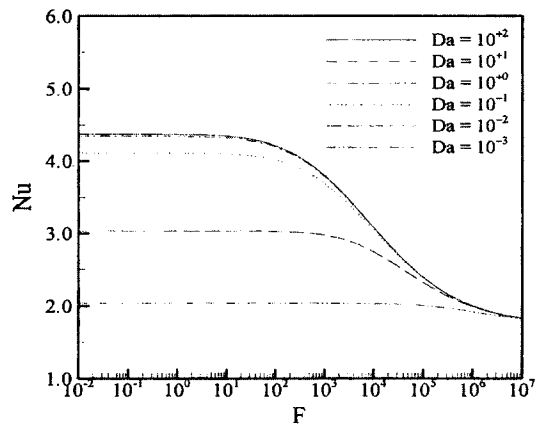
affected significantly by the existence of the layer, and, therefore, T_m increases more rapidly than T_w as the porous layer thickness increases. As a result, the temperature difference ($T_w - T_m$) decreases, which results in the increase of the Nu as compared to the porous layer free case. The average temperature rise becomes more remarkable up to a critical thickness of the layer. Upon further increasing of the layer thickness, however, T_m has weaker dependence on the thickness, hence the temperature difference ($T_w - T_m$) increases after the critical thickness of the layer has been reached and, as a result, Nu begins to decrease. Notice that when the pipe is fully filled with a porous medium ($R/R_o=1$), Nu is 8.00 (Nield and Bejan, 1992) as $Da \rightarrow 0$. Note also Nu becomes the well-known value of 4.36 (Bejan, 1995) as $Da \rightarrow \infty$ for fully developed pipe flow. As expected, the effect of the porous layer diminishes as Da increases, i.e., permeability increases. The maximum value of Nu shifts to the left as Da increases. This result implies that the critical thickness of the porous layer, where T_m begins to increase slower than T_w , becomes smaller for higher permeability porous media.

Figure 4(c) illustrates Nu for Case I with constant wall temperature boundary condition. Nu is generally smaller than for the constant-flux boundary case. As shown in Fig. 4(c), the dependence of Nu on the porous layer thickness and Da for the constant wall temperature case is qualitatively similar to that of the constant wall heat flux case. As a result, this trend is expected to continue for the other parameters used. We investigated the effects of various parameters for the constant wall heat flux case.

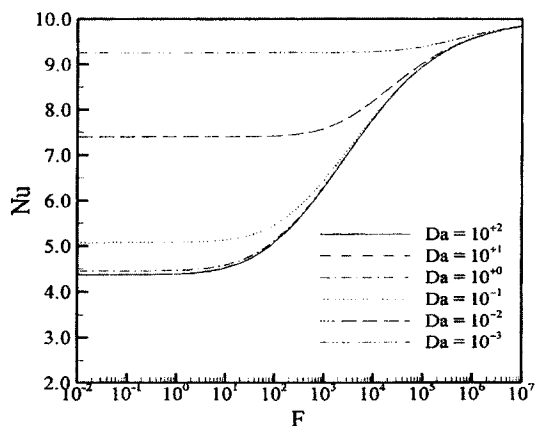
The effect of F for various Da with $R_\mu=1$ is shown in Fig. 5. In accord with the asymptotic result, as shown in Fig. 5(a), Nu shows a tendency toward the slug flow value of 8.00 for the fully porous layer case. Here, Nu increases with F . However, the Nu dependence on Da becomes smaller as F increases. The values of Nu in Case II ($R/R_o=0.5$) are larger than those of the fully-porous case for all values of Da and F , and the difference in Nu becomes significant



(a)



(b)



(c)

Fig. 5 Effect of F on the Nusselt number for constant wall heat flux with $R_\mu=1$: (a) fully porous case, (b) Case I ($R/R_o=0.5$), and (c) Case II ($R/R_o=0.5$)

as Da decreases. However, this is just a coincidence since Nu depends not only on Da but also on the thickness of the porous layer, as shown in Fig. 4. It is worth noting that Nu decreases with permeability for Case I with $R/R_0=0.5$ (Fig. 5 (b)), which is the reverse of the trend shown in the fully porous case (Fig. 5 (a)) and Case II with $R/R_0=0.5$ (Fig. 5(c)).

The effect of F in Fig. 6 is qualitatively equivalent to decreasing the permeability of the porous layer (i.e. shown in Fig. 2). As F increases, the velocity profiles are flattened, as shown in Fig. 6. However, the shape of the temperature distribution does not always sharpen as F increases. Rather, it depends on the geometry and porous layer thickness as shown in Fig. 7. For Case I with $R/R_0=0.5$ (Fig. 7(b)), the increase of F causes a flattening, not a sharpening, of the temperature distribution shape, contrary to the other cases (Figs. 7(a) and (c)). However, for the fully porous layer case, an increase in F always results in sharpening of the temperature profiles for the parameter range we studied, which is the result obtained by Nield et al.(1996).

Figure 8 shows the effect of F on Nu for $R_\mu=0.1, 1$ and 10 , respectively. For all values of R_μ , Nu increases with F for the fully porous case and Case II ($R/R_0=0.5$) as shown in Figs. 8(a) and (c). This is because an increase in F causes the flow to be more slug-type; hence the temperature difference decreases resulting in an increase in Nu . In the Case I ($R/R_0=0.5$), however, Nu decreases as the drag increases. The explanation for this result is given by examining the effect of porous layer on T_w . When the porous layer is attached at the wall, it is expected that the wall temperature will be affected more significantly than T_m by the existence of a porous layer. As a result, the temperature difference increases, and thus Nu decreases.

Predicting the effect of the R_μ on Nu is not straightforward. As R_μ varies from 1 to 10 , Nu increases for all values of F for the fully porous case (Fig. 8(a)), while there is no such trend in Case I ($R/R_0=0.5$) and Case II ($R/R_0=0.5$), as shown in Figs. 8(b) and (c). Generally, the velocity profile varies considerably with R_μ as

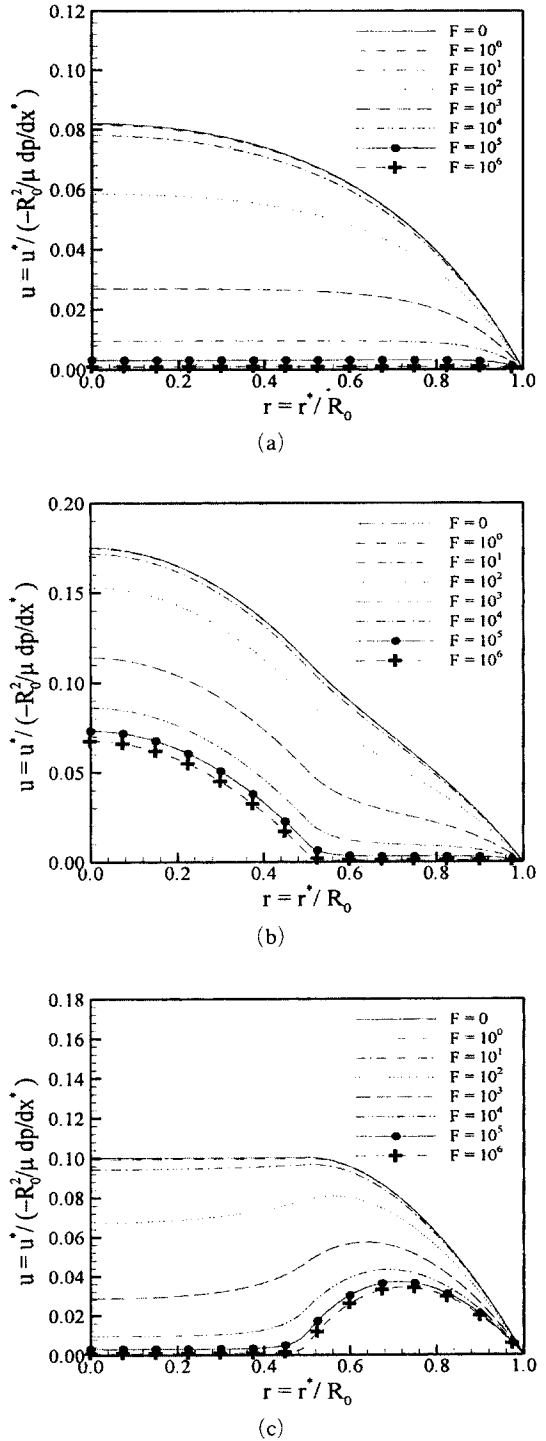


Fig. 6 Effect of F on the velocity for constant wall heat flux with $R_\mu=1$ and $Da=0.1$: (a) fully porous case, (b) Case I ($R/R_0=0.5$), and (c) Case II ($R/R_0=0.5$)

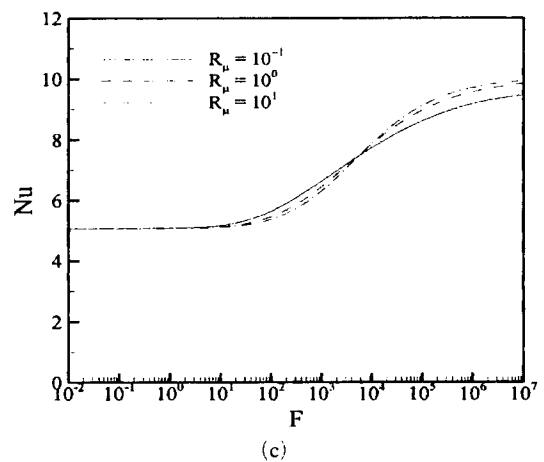
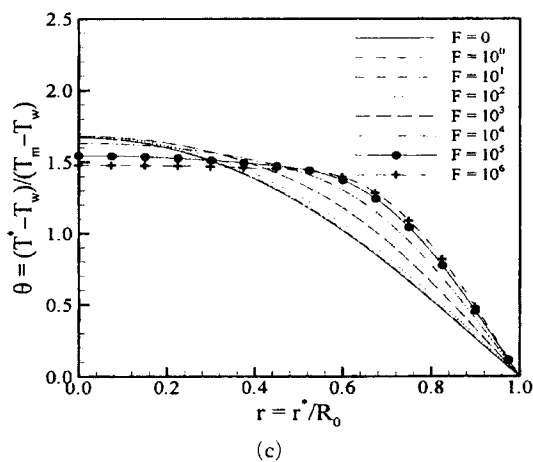
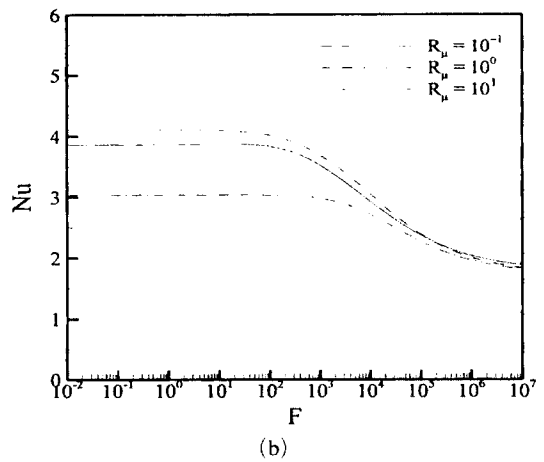
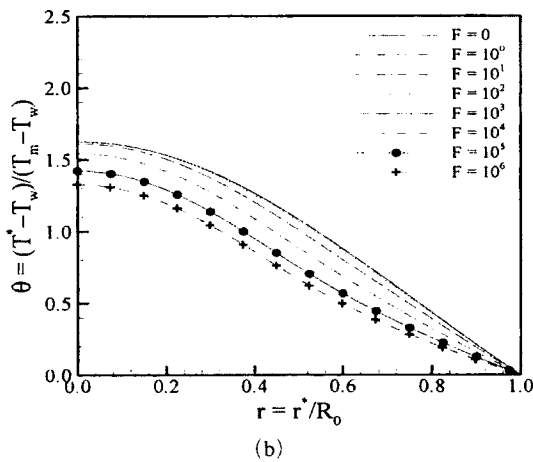
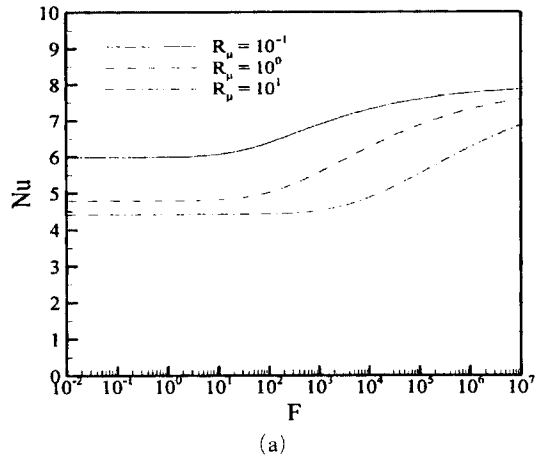
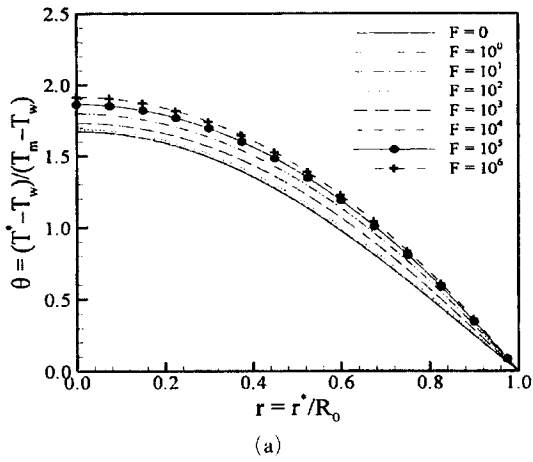
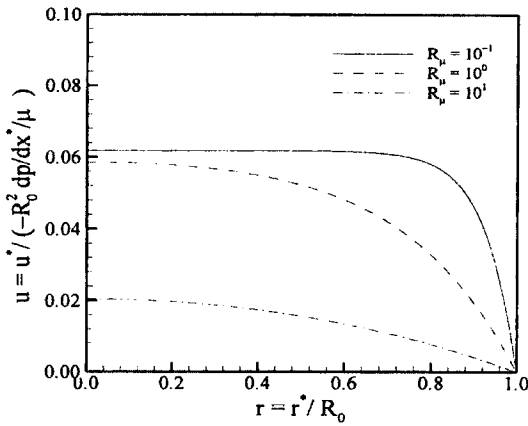
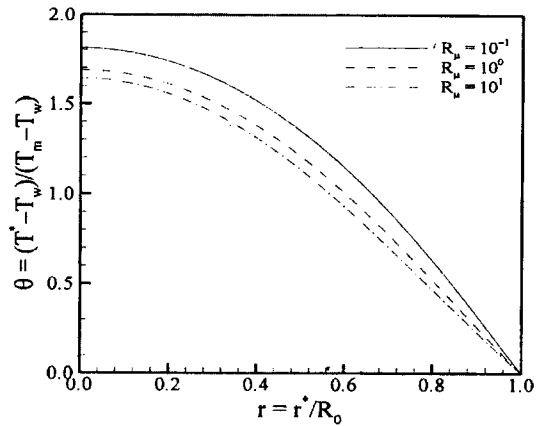


Fig. 7 Effect of F on the temperature profile for constant wall heat flux with $R_\mu=1$ and $Da=0.1$: (a) fully porous case, (b) Case I ($R/R_0=0.5$), and (c) Case II ($R/R_0=0.5$)

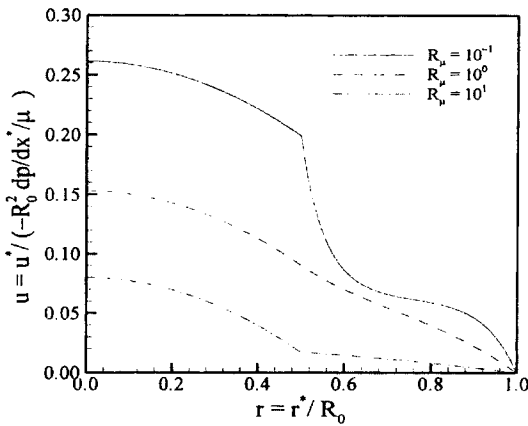
Fig. 8 Effect of R_μ and F on the Nu for constant wall heat flux with $Da=0.1$: (a) fully porous case, (b) Case I ($R/R_0=0.5$), and (c) Case II ($R/R_0=0.5$)



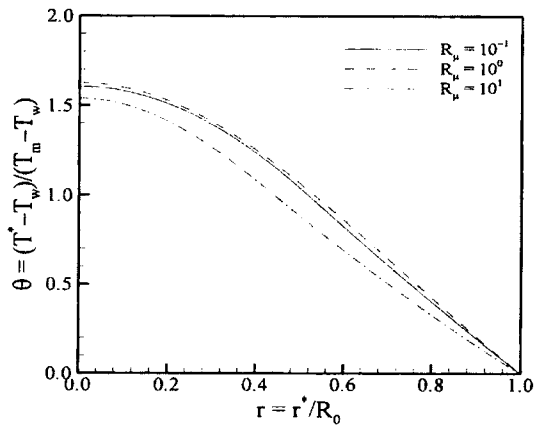
(a)



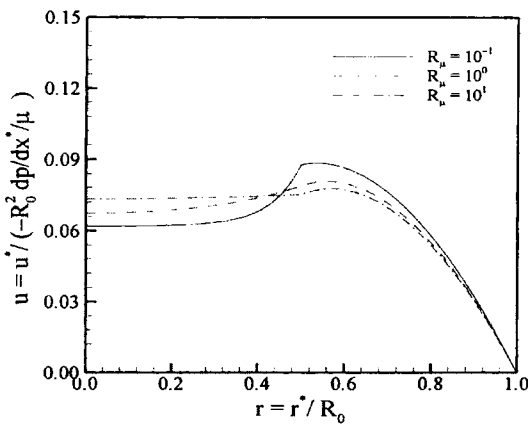
(a)



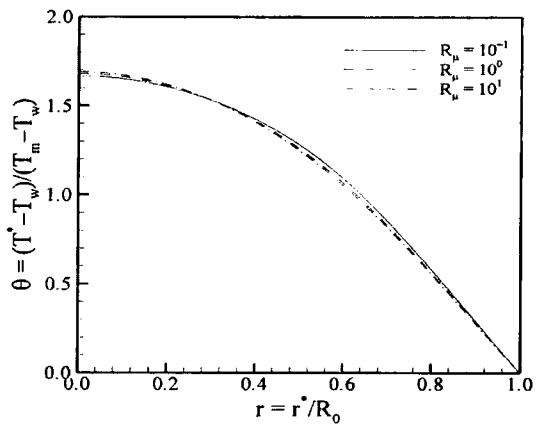
(b)



(b)



(c)



(c)

Fig. 9 Effect of R_μ on the velocity profile for constant wall heat flux with $Da=1$ and $F=10^2$: (a) fully porous case, (b) Case I ($R/R_0=0.5$), and (c) Case II ($R/R_0=0.5$)

Fig. 10 Effect of R_μ on the temperature profile for constant wall heat flux with $Da=1$ and $F=10^2$: (a) fully porous case, (b) Case I ($R/R_0=0.5$), and (c) Case II ($R/R_0=0.5$)

plotted in Fig. 9, but the temperature profiles are not significantly affected by R_μ , as is shown in Fig. 10. For $R_\mu \neq 1$, the velocity profiles show steep changes at $R/R_0=0.5$ due to the shear stress matching condition (Eq. (7)). The shear rate is not continuous, although the shear stress is continuous at $R/R_0=0.5$. The dependence of Nu on R_μ and the thickness of the porous layer, as well as on Da , are shown in Fig. 11, which demonstrates that Nu does not depend on R_μ directly for either Case I or Case II.

The effect of R_k on Nu is plotted in Figs. 12 (a) and (b), which show that Nu increases with R_k , and Nu linearly depends on R_k for the fully-porous case. As the thickness of the porous layer

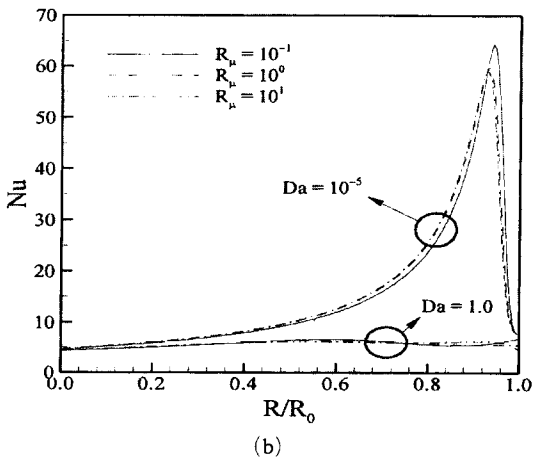
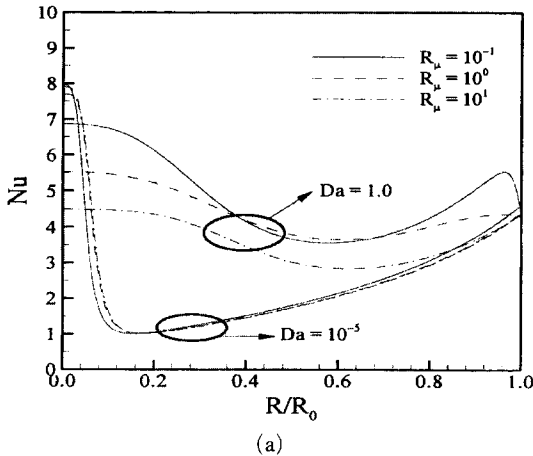


Fig. 11 Effect of Da and R_μ on Nu for constant wall heat flux for $F=10^3$: (a) Case I and (b) Case II

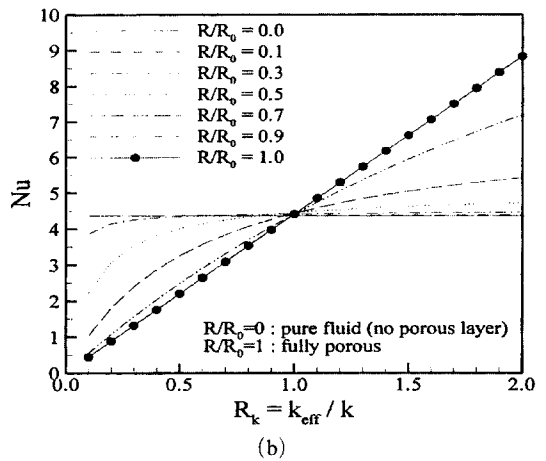
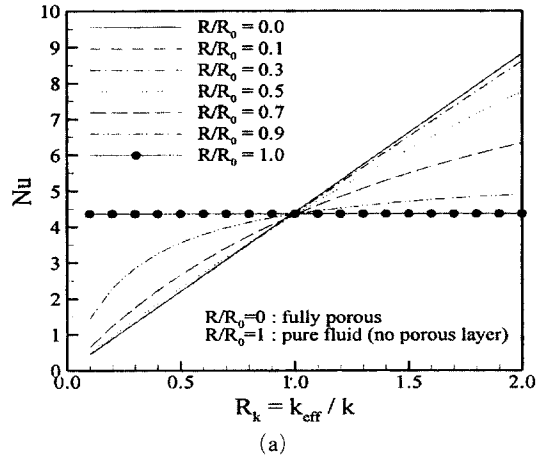


Fig. 12 Effect of R_k on Nu for constant wall heat flux for $F=0$, $Da=0.1$, and $R_\mu=1$: (a) Case I and (b) Case II

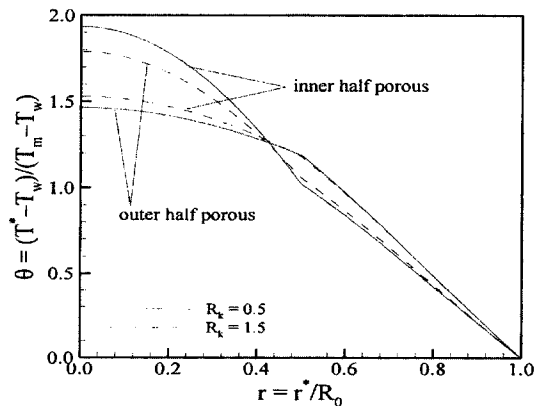


Fig. 13 Effect of R_k on the temperature profiles for constant wall heat flux for $F=0$, $Da=0.1$, and $R_\mu=1$

decreases, the dependence of Nu on R_k becomes nonlinear. It is worth noting that for the half porous layer ($R/R_0=0.5$), Nu of Case II is larger than of the Case I for $R_k < 1$. However, for $R_k > 1$, Nu of Case I is greater than that of Case II. For $R_k < 1$, the average temperature of Case II is larger, as shown in Fig. 13, and thus the $(T_w - T_m)$ becomes smaller. Therefore, Nu for Case II is larger than the Nu for Case I. The reverse trend appears for $R_k > 1$.

5. Conclusions

The forced convection in a circular pipe with a partially filled porous medium was numerically investigated. Two types of configurations (inner and outer porous layer denoted as Cases I and II) were investigated for various parameters, including the Darcy number, the thickness of porous layer, and the ratio of the viscosity & thermal conductivity of the porous medium to those of the fluid. The results are summarized as follows:

(1) Nu dependence on the thickness of the porous medium is not uniform. There exists a critical porous layer thickness where the Nu reaches a maximum for Case II and reaches a minimum for Case I for any Darcy number.

(2) Nu increases with Forchheimer number for the fully porous case and Case II ($R/R_0=0.5$). For the Case I ($R/R_0=0.5$), Nu decreases as Forchheimer number increases.

(3) Nu increases with the viscosity ratio. The effect of the viscosity ratio on the Nu is not simple, since Nu depends also on Darcy number, the porous layer thickness, the configuration of the layer, as well as on the viscosity ratio.

(4) For a given porous layer thickness, the value of Nu depends on the type of porous layer configuration.

References

- Ahmadi, G. and Smith, D. H., 2002a, "Gas Flow and Particle Deposition in the Hot-Gas Filter Vessel of the Pinon Pine Project," *Powder Technology*, Vol. 128, No. 1, pp. 1~10.
- Ahmadi, G. and Smith, D. H., 2002b, "Analysis of Steady-state Filtration and Backpulse Process in a Hot-Gas Filter Vessel," *Aerosol Science and Technology*, Vol. 36, No. 6, pp. 665~677.
- Ahmadi, G. and Smith, D. H., 1998, "Particle Transport and Deposition in a Hot-Gas Cleanup Pilot Plant," *Aerosol Science and Technology*, Vol. 29, No. 3, pp. 183~205.
- Back, Y. R., Chung, D. K., Jeong, H. I., Kang, S. C. and Jhon, M. S., 1997, "Permeability Effects of the Ceramic Candle Filter on Back-pulse Cleaning System," *KSME International Journal*, Vol. 11, No. 3, pp. 359~366.
- Bejan, A., 1995, *Convective Heat Transfer*, Wiley, New York, NY.
- Ethier, C. R. and Kamm, R. D., 1989, "Flow Through Partially Gel-filled Channels," *Physicochemical Hydrodynamics*, Vol. 11, pp. 219~227.
- He, W., Yi, J. S. and Nguyen, T. V., 2000, "Two-Phase Flow Model of the Cathode of PEM Fuel Cells Using Interdigitated Flow Fields," *AIChE Journal*, Vol. 46, pp. 2053~2064.
- Jeong, Y. S., Lee, S. M., Kim, N. K., Hwang, J. M. and Chae, J. O., 1998, "A Study on Combustion Characteristics of Superadiabatic Combustor in Porous Media," *KSME International Journal*, Vol. 12, No. 4, pp. 680~687.
- Kaviany, M., 1985, "Laminar Flow Through a Porous Channel Bounded by Isothermal Parallel Plates," *International Journal of Heat and Mass Transfer*, Vol. 28, pp. 851~858.
- Mckenzie, P. F., Kapur, V. and Anderson, J. L., 1994, "Effects of Adsorbed Homopolymer and Diblock Copolymer on Molecular-Transport in Micropores," *Colloids and Surfaces A*, Vol. 86, pp. 263~274.
- Nguyen, T. V. and He, W., 2002, Interdigitated Flow Field Design: Experimental Results and Theoretical Calculations, *In Handbook of Fuel Cell Technology: Fuel Cell Technology and Applications, Volume III* (Edited by Vielstich, W., Gasteiger, H., and Lamm, A.), Wiley, New York, NY.
- Nield, D. A. and Bejan, A., 1992, *Convection in Porous Media*, Springer, New York, NY.
- Nield, D. A., Junqueira, S. L. M. and Lage, J. L., 1996, "Forced Convection in a Fluid-

Saturated Porous-Medium with Isothermal or Isoflux Boundaries," *Journal of Fluid Mechanics*, Vol. 322, pp. 201~214.

Poulikakos, D. and Kazmierczak, M., 1987, "Forced Convection in a Duct Partially Filled with a Porous Material," *ASME Journal of Heat Transfer*, Vol. 109, No. 3, pp. 653~662.

Poulikakos, D. and Renken, K., 1987, "Forced Convection in a Channel Filled with Porous Medium, Including the Effects of Flow Inertia, Variable Porosity, and Brinkman Friction,"

ASME Journal of Heat Transfer, Vol. 109, No. 4, pp. 880~888.

Vafai, K. and Kim, S. J., 1989, "Forced Convection in a Channel Filled with a Porous Medium: An Exact Solution," *ASME Journal of Heat Transfer*, Vol. 111, pp. 1103~1106.

Webber, R. M., Anderson J. L. and Jhon, M. S., 1990, "Hydrodynamic Studies of Adsorbed Diblock Copolymers in Porous Membranes," *Macromolecules*, Vol. 23, No. 4, pp. 1026~1034.